



Cite this: *RSC Mechanochem.*, 2025, 2, 240

Mechanochemical generation of nitrogen-centred radicals for the formation of tertiary amines in polymers†

Sonja Storch, ^{ab} Davide Campagna, ^{ab} Simay Aydonat ^{abc} and Robert Göstl ^{abc}

Force-activated functional groups in polymers may inform the design of future smart materials in which mechanical events trigger productive chemistry. The availability of such mechanochemically active tools (mechanophores) is perpetually increasing, but the limited understanding of mechanochemical reactivity complicates the identification of new molecular motifs that render reactive groups accessible by force. Here, we expand the chemical scope of our previously reported carbamoyloxime mechanophore motif from latent secondary to tertiary amines by harnessing the reactivity of transient nitrogen-centred radicals formed in the mechanochemical reaction pathway. Carbamoyloximes are modified with an *N*-pentenyl substituent which undergoes a consecutive intramolecular 5-exo-trig ring-closing reaction with an aminyl radical generated upon force-induced homolytic scission of the mechanophore, thereby enabling the hitherto unexplored mechanochemical activation of latent tertiary amines. We therefore show that carbamoyloxime mechanophores are nitrogen-centred mechanoradical generators expanding the chemical space of polymer mechanochemistry.

Received 5th September 2024
Accepted 12th December 2024

DOI: 10.1039/d4mr00099d
rsc.li/RSCMechanochem

Introduction

Mechanophores introduce latent functionality in polymers and can be activated on demand by mechanical force.¹ Thereby, they convert molecular bond scission into programmed productive responses.^{2–6} For example, mechanophores have enabled force-induced polymerizations,^{7,8} the optical detection of force-induced events,^{9,10} mechanochemical recycling,^{11,12} and sonopharmacology,^{13,14} which motivates underlying fundamental research on new derivatives.

To date, the activation or release of a variety of chemical functionalities has been reported including acids,^{15–17} active metal centres,^{18–22} carbenes,²³ and persistent radicals.^{24,25} However, the discovery of new force-accessible functional groups remains complicated due to a limited understanding of mechanochemical reactivity.^{26,27} Consecutive cascade reactions of mechanochemically generated transient species are hence a plausible strategy to increase the accessible chemical space using available mechanophores.²⁸ This has been demonstrated for simple moieties, such as azo or disulfide bonds, which

undergo homolytic cleavage under force.^{29,30} For example, the highly reactive radical species resulting from azo bond cleavage have been used for self-amplifying downstream processes, such as polymerization and self-immolation,^{31,32} or sonopharmacology.³³ Disulfide breakage, on the other hand, generates a thiol radical and subsequently a thiol whose nucleophilic character has been used to induce intramolecular cyclization reactions, for payload release from carbonates and carbamates.^{34–36}

Other concepts have been developed to enable the mechanochemical activation of primary amines through hydrolysis of imine functions generated from aziridines³⁷ or through the release of small molecules from latent carbamates.^{36,38–41} Moreover, we have recently achieved the activation of a chemically useful secondary amine using carbamoyloxime mechanophores.⁴² While latent mechanoresponsive primary and secondary amines for the incorporation into polymers are thus available, tertiary amines are still lacking despite their broad use as organic bases or organocatalysts for polymer-related applications, such as the synthesis of epoxy resins,⁴³ polyurethanes,⁴⁴ or vitrimers.⁴⁵

The underlying challenge of the mechanochemical activation of latent tertiary amines is the requisite mechanophore bond scission. Therefore, generating tertiary amines by simply using one of the established pathways for mechanochemical amine generation with an adjusted number of *N*-substituents is either not possible in the case of the aziridine mechanophore given the hydrolysis step that furnishes the amine, or would correspond to a hypothetical carbamate of a quaternary ammonium ion, which does not exist.

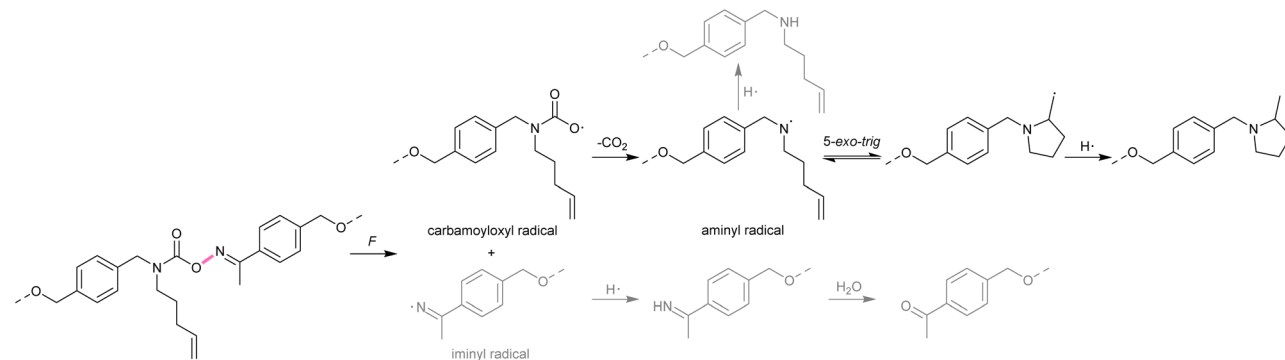
^aDWI – Leibniz Institute for Interactive Materials, Forckenbeckstr. 50, Aachen 52056, Germany. E-mail: goestl@uni-wuppertal.de

^bInstitute of Technical and Macromolecular Chemistry, RWTH Aachen University, Worringerweg 2, Aachen 52074, Germany

^cDepartment of Chemistry and Biology, University of Wuppertal, Gaußstr. 20, Wuppertal 42119, Germany

† Electronic supplementary information (ESI) available. See DOI: <https://doi.org/10.1039/d4mr00099d>



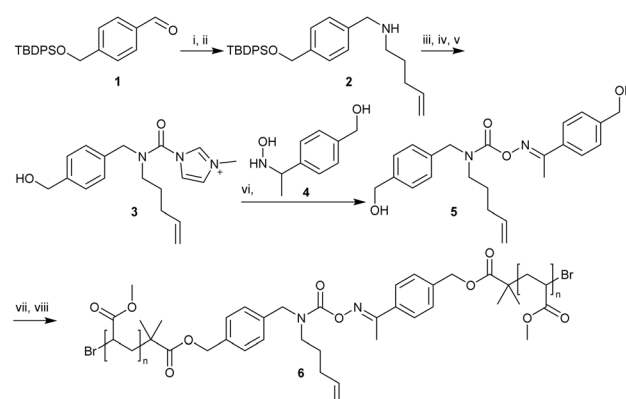


Scheme 1 Mechanochanical activation and subsequent 5-exo-trig cyclization of modified carbamoyloxime mechanophore for the generation of a tertiary amine. Dashed bonds signify attachment points to the polymer structure. The initially broken covalent bond is shown in pink.

Here, we demonstrate the mechanochemical activation of a latent tertiary amine through a reaction pathway of a suitably modified carbamoyloxime mechanophore. Therefore, we exploit the formation of reactive transient nitrogen-centred radicals to enable a consecutive intramolecular ring-closing reaction (Scheme 1). The mechanochemical reaction pathway of carbamoyloximes has been investigated by us previously.^{42,46} Overstretching induces homolytic N–O bond scission, which on the one side produces an iminyl radical that reacts to an imine function and subsequently hydrolyzes to a ketone if the α -substituent is not H. The transient carbamoyloxy radical formed on the other side decarboxylates to give an aminyl radical, which can take up an H-atom to afford a secondary amine. Nitrogen-centred radical species are considered versatile synthons for the construction of N-heterocycles due to their reactivity toward sp^2 -systems, yielding, *e.g.*, lactams, pyridines, quinolines, or pyrrolidines.^{47,48} One important pathway toward nitrogen-containing cyclic moieties are intramolecular ring-closing reactions yielding the kinetically preferred *exo*-product.⁴⁹ The reaction rate hereby depends on the nucleophilicity of the respective nitrogen-centred radical, which in the case of aminyl radicals leads to a significant increase in reaction rate for the protonated aminium radical.^{47,50} Additionally, hydrogen atom donors (HAD) can be employed to terminate the forming cyclic carbon radical species, shifting the equilibrium to the product side.^{47,50} Here, we make use of the aminyl radical species formed upon activation of the carbamoyloxime mechanophore for a consecutive intramolecular 5-exo-trig ring-closing reaction,⁵¹ thereby demonstrating the unprecedented mechanochemical activation of latent tertiary amines in polymers.

Results and discussion

Key structural modification to enable the targeted intramolecular 5-exo-trig cyclization was the incorporation of an *N*-pentenyl substituent. The recently established carbamoyl methylketoxime (MKO) mechanophore derivative was chosen given its superior mechanochemical kinetics as well as thermal and UV resistance and facile synthesis (Scheme 2).⁴⁶ Reductive amination of protected 4-(hydroxymethyl) benzaldehyde **1** furnished secondary amine **2**, from which the synthesis was



Scheme 2 Synthesis of *N*-pentenyl-substituted carbamoyl methylketoxime incorporated in linear PMA. (i) 4-Pentenylamine, MeOH, N_2 , r.t., 3 h. (ii) $NaBH_4$, N_2 , 0 °C to r.t., 30 min. (iii) CDI, Et_3N , THF, N_2 , 60 °C, overnight. (iv) TBAF, THF, N_2 , 0 °C to r.t., 30 min. (v) MeI , Et_3N , MeCN, N_2 , r.t., 36 h. (vi) Et_3N , MeCN, N_2 , r.t., overnight. (vii) α -Bromo isobutyryl bromide, Et_3N , THF, N_2 , 0 °C to r.t., overnight. (viii) Methyl acrylate, Cu^0 , $CuBr_2$, Me₆TREN, Ar, r.t., 6 h.

carried out analogously to the established procedure for MKO. Carbamoylating the amine function of **2** using carbonyldiimidazole (CDI), followed by deprotection of the hydroxyl group and methylation of the imidazole rendered the carbamoyl imidazolinium salt **3** susceptible to coupling with ketoxime **4**, thus affording the carbamoyl methylketoxime diol **5**. Cu^0 -mediated controlled radical polymerization was used to incorporate **5** into the centre of linear poly(methyl acrylate) (PMA) chains, yielding the polymer **6** ($M_n = 90$ kDa, $D_M = 1.3$). The thermal stability of **5** was assessed by ¹H NMR in DMSO-d₆ at 130 °C for 24 h (Fig. S2†), found to correspond to the heat tolerance of unmodified MKO, and thus remained unaffected by the structural changes.

Subsequently, we analyzed the mechanochemical scission kinetics of **6**. Despite introducing the *N*-pentenyl substituent in a location distant to the initial mechanochemical bond scission site, we evaluated potential deviations between the N–O bond of MKO and **6**. Therefore, we performed CoGEF^{26,52} simulations which qualitatively suggested a probable activation of the targeted N–O bond (Fig. S1†).



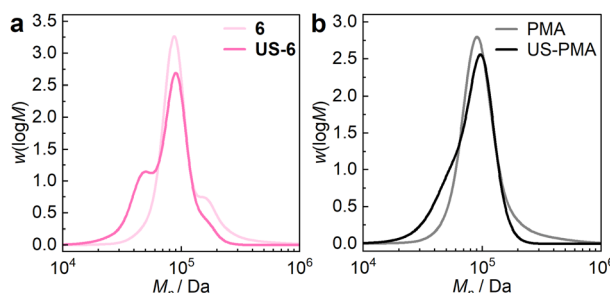


Fig. 1 Mechanochemical activation after US (20 kHz, 30% amplitude, 1 : 1 s pulse, 30 min) of (a) **6** in comparison to (b) pristine PMA without mechanophore ($M_n = 88$ kDa, $D_M = 1.3$). MMDs obtained by gel permeation chromatography (GPC) with refractive index detector in THF relative to a PMMA standard.

Furthermore, we successfully verified the accelerated bond scission of **6** subjected to ultrasound (yielding **US-6**) using an immersion probe sonicator at 20 kHz. We compared the apparent scission rate to pristine PMA (Fig. 1) and determined an average mechanochemical selectivity of bond scission of 40% (Table S4†), which is comparable to our previously reported carbamoyloxime mechanophores.^{42,46}

The molar mass distribution (MMD) of **6** showed a shoulder toward higher M which could possibly arise from bimolecular termination during the polymerization. However, the same shoulder appeared in all MMDs obtained after repeating the polymerization of **6** (Fig. S40†). We therefore suspected the fractional incorporation of the *N*-pentenyl substituent double bond. This was further supported by the uniform MMD of a control carbamoyloxime mechanophore polymer **c6** that featured an aliphatic *N*-substituent (Fig. S28†). This issue could potentially be resolved by identification of a monomer that would undergo stronger ideal, non-azeotropic copolymerization with the pentenyl moiety. Since, however, the monomer choice was limited to ensure efficient force transmission during ultrasonication^{53,54} and the loss of the double bond was not within the detectable range of ¹H NMR analysis (Fig. S39†), we considered the amount of incorporated double bond to have a negligible impact.

We then investigated the targeted 5-*exo-trig* cyclization upon activation of **6** by US. As described above, addition of a weak

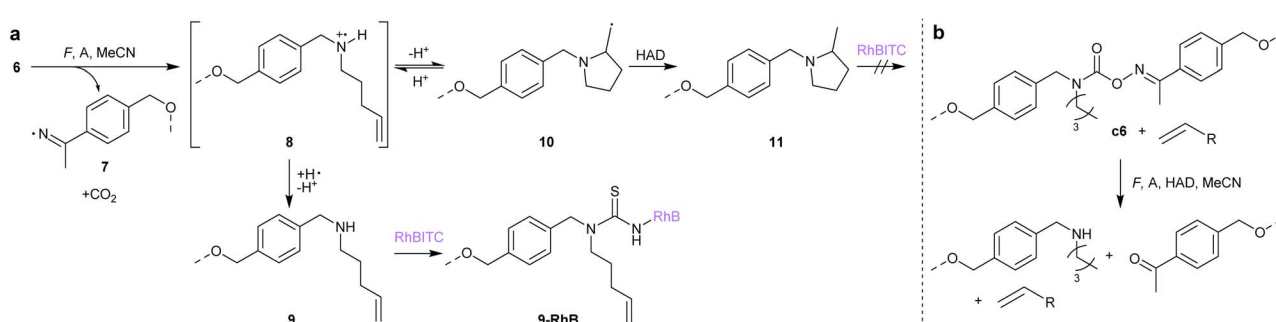
acid enhanced the reactivity by protonating the aminyl radical and a suitable HAD trapped the ring-closed carbon radical **10** (Scheme 3a). Ultrasonication of **6** was therefore carried out in different conditions: without the addition of additives (Table 1, entries 1a–c), in presence of malonic acid (A, Table 1, entries 2a–c), and in presence of A and 1–4 cyclohexadiene (CHD) as HAD (Table 1, entries 3a–c). Each experiment was analyzed by GPC and ¹H NMR spectroscopy and the overall fraction of polymer chain scission *f*, the chain scission selectivity for mechanophore activation *S*, the fraction of activated mechanophore *x_{act}*, and the fractional decrease of the *N*-pentenyl double bond in the formed products *x_d* were determined (Tables 1, S4, and S5†). To exclude any potential uncontrolled chemical transformation or degradation of the mechanophore, specifically, the *N*-pentenyl double bond, in the presence of A and CHD during ultrasonication, we verified the stability of the small molecule **5** toward acidic environment (Fig. S3†) as well as during ultrasonication of pristine PMA in the presence of A and CHD (Fig. S5†).^{48,50}

Considering the reaction pathway of the (protonated) aminyl radical **8**, two scenarios were possible: (i) cyclization and formation of the tertiary amine **11**. (ii) No cyclization yielding the secondary amine **9**. Other cyclization modes using aminyl or

Table 1 Fraction of scission *f*, selectivity *S* of the mechanochemical reaction, overall fraction of activated mechanophore *x_{act}*, and fractional decrease of the double bond *x_d*

Entry	Reactants	<i>f</i> ^a	<i>S</i> ^{a,b} /%	<i>x_{act}</i> ^b	<i>x_d</i> ^b
1a	6	1.58	29	0.46	0.45
2a	6 + A	1.36	31	0.42	0.77
3a	6 + A + HAD	1.09	36	0.40	0.99
1b	6	0.99	33	0.33	0.48
2b	6 + A	1.04	38	0.40	0.81
3b	6 + A + HAD	1.14	43	0.50	1.13
1c ^c	6	0.78	45	0.35	0.64
2c ^c	6 + A	0.87	50	0.44	0.93
3c ^c	6 + A + HAD	0.91	49	0.45	1.10
3d ^c	c6 + A + HAD + olefin	0.76	42	0.35	0

^a Determined by GPC. ^b Determined by ¹H NMR. ^c NMR spectra shown in Fig. 3.



Scheme 3 (a) Mechanochemical reaction pathways of **6** in presence of A and HAD. Secondary amines formed during the reaction were visualized through the selective labelling with RhBITC after workup. (b) Mechanochemical activation of control carbamoylketoxime **c6** lacking vinyl functionality for cyclization with added vinyl control.



aminium radicals are kinetically unlikely.^{47,48} Evaluating the products of this reaction thus posed a challenge as it required the differentiation between a chain-terminal secondary and tertiary amine. We employed Rhodamine B isothiocyanate (RhBITC) as selective labelling agent for secondary amines being unreactive towards tertiary amines⁵⁵ (Fig. S7†) to treat **6** after US (Scheme 3a). This allowed to compare the fraction of secondary amine formed in different reaction conditions.

Comparing the relative UV absorption by GPC of RhBITC-treated **US-6** with and without addition of A and HAD, respectively, elucidated the influence of cyclization-promoting additives on the amount of formed secondary amine **9** during the mechanochemical reaction. **US-6** was washed with 1 M aqueous NaOH solution prior to the reaction with RhBITC to receive amines instead of ammonium salts formed due to the presence of A during sonication, and a threefold determination was performed (Fig. 2). Addition of A decreased the degree of functionalization with RhB and even more so when HAD was added, indicating diminished competing formation of secondary amines in reaction conditions favorable for the *5-exo-trig* cyclization.

Direct analysis of **11** by ¹H NMR *via* the 2-methylpyrrolidine moiety that could be distinguished from the signals of **9** was hampered due to overlapping polymer backbone signals. Tertiary amine formation could however be estimated from diagnostic changes in observable signals of carbamoyloxime moieties before and after mechanochemical activation. Fig. 3a shows the included aromatic protons of starting material **6**, the iminyl pathway products (imine and ketone function) accounting for the amount of activated **6**, and the vinylic proton of the *N*-pentenyl substituent, for which the chemical shift was the same before (**6**) and after (**9**) mechanophore cleavage (Fig. S36†), unless the double bond was consumed during cyclization.

To ensure that the double bond only reacted during cyclization, a control mechanophore **c6** with *N*-alkyl substituent to prevent intramolecular ring-closing was incorporated into linear PMA (Scheme 3b) and ultrasonicated in cyclization-promoting conditions along with a small molecule vinyl control (Table 1, entry 3d). After sonication, the double bond of

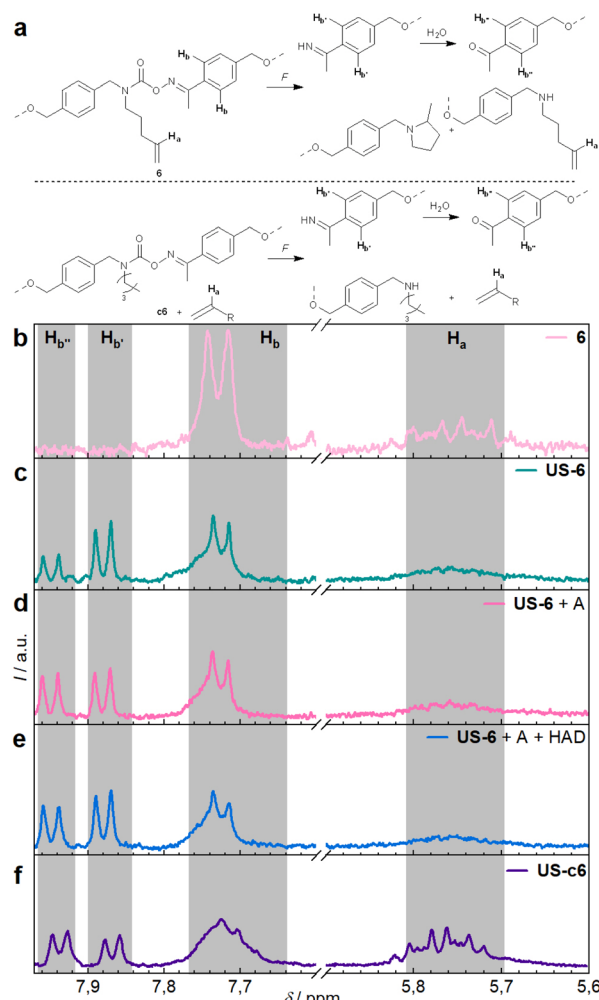


Fig. 3 ¹H NMR analysis of the mechanochemical reaction of **6**. (a) Scheme denoting all measured protons. From top to bottom ¹H NMR spectra corresponding to (b) starting material **6**, (c) **US-6** (Table 1, entry 1c), (d) **US-6 + A** (Table 1, entry 2c), (e) **US-6 + A + HAD** (Table 1, entry 3c), and (f) control **US-c6** (Table 1, entry 3d).

the vinyl control was found unaltered, indicating absence of a competing intermolecular reaction (Fig. 3f). Thus, the intramolecular *5-exo-trig* cyclization for ultrasonicated **6** could be monitored by the decrease of the vinylic proton signal of the *N*-pentenyl substituent. Upon ring-closing, the double bond would react to tertiary amine **11** and the corresponding vinylic proton signal therefore would disappear, whereas if no cyclization would take place, secondary amine **9** would form, and the signal would remain unchanged. The decrease of the double bond upon mechanochemical activation was therefore quantified by ¹H NMR (Table 1) using the signal integrals of remaining starting material **6** (Fig. 3, H_{b}), products from the iminyl pathway (H_{b}' and H_{b}''), and double bond signal (H_{a}).

The decrease of the double bond followed the expected reactivity trend of the *5-exo-trig* cyclization: no additives $< \text{A} < \text{A} + \text{HAD}$ (Table 1), which was in accordance with and reinforced the results of the previous RhBITC-labelling experiment. The measured values $x_{\text{d}} > 1$ were attributed to the limited sensitivity

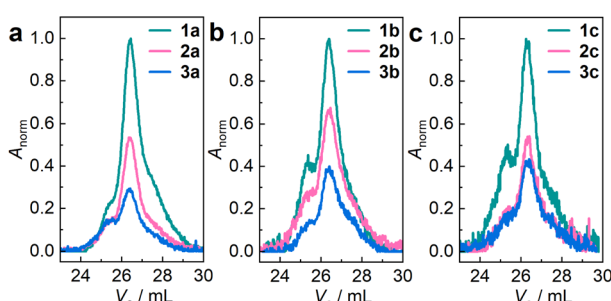


Fig. 2 (a–c) GPC elograms in THF with UV-vis detector of 9-RhB after sonication in triplicate with different additives. Annotations in the legends of the graphs are referenced to the entries in Table 1. Absorption was normalized and corrected by the fraction of activated mechanophore x_{act} .



and resolution of NMR measurements toward polymer end groups and suggested a slight general overestimation of the determined values. However, the qualitatively observed overall reactivity trend was validated with the consistent threefold determinations which yielded significantly differing x_d depending on the employed reaction conditions. Since the control experiments excluded significant side reactions in which the double bond function was involved, its consumption during irradiation with US was plausibly traced back to mechanochemically induced ring-closing, yielding **11** as tertiary amine.

Conclusions

Carbamoyloxime mechanophores undergo force-induced homolytic cleavage at the N–O bond, which triggers a radical cascade culminating in the formation of secondary amine on the one side, and nitrile, imine, and ketone polymer end groups on the other side. Here, we expanded the chemical scope of this mechanophore class by using the transient nitrogen-centred aminyl radicals to enable a consecutive 5-*exo-trig* cyclization reaction for the mechanochemical, additive-supported activation of a latent tertiary amine. In the future, more accurate tertiary amine-selective measurements may allow a more detailed interpretation of the underlying mechanism. Nevertheless, the herein presented approach of exploiting carbamoyloxime mechanophores as modifiable platform for nitrogen-centred mechanoradical chemistry holds promise for future research on the chemical versatility of this mechanophore class.

Data availability

All data of this study are documented within the manuscript and its ESI† and are publicly available in Zenodo at <https://doi.org/10.5281/zenodo.13365256>.

Author contributions

S. S.: methodology; validation; formal analysis; investigation; data curation; writing – original draft, writing – review & editing. D. C.: conceptualization; methodology. S. A.: methodology. R. G.: resources; writing – review & editing; supervision; project administration; funding acquisition.

Conflicts of interest

There are no conflicts to declare.

Acknowledgements

Funding is acknowledged from the German Research Foundation for 503981124 (R. G.) and 508998124 (R. G., S. S.) as well as from the Federal Ministry of Education and Research for 031B1148A (R. G., S. A.).

Notes and references

- Y. Chen, G. Mellot, D. van Luijk, C. Creton and R. P. Sijbesma, *Chem. Soc. Rev.*, 2021, **50**, 4100–4140.
- B. A. Versaw, T. Zeng, X. Hu and M. J. Robb, *J. Am. Chem. Soc.*, 2021, **143**, 21461–21473.
- E. M. Lloyd, J. R. Vakil, Y. Yao, N. R. Sottos and S. L. Craig, *J. Am. Chem. Soc.*, 2023, **145**, 751–768.
- M. A. Ghanem, A. Basu, R. Behrou, N. Boechler, A. J. Boydston, S. L. Craig, Y. Lin, B. E. Lynde, A. Nelson, H. Shen and D. W. Storti, *Nat. Rev. Mater.*, 2021, **6**, 84–98.
- N. Willis-Fox, E. Rognin, T. A. Aljohani and R. Daly, *Chem.*, 2018, **4**, 2499–2537.
- R. Küng, R. Göstl and B. M. Schmidt, *Chem. Eur. J.*, 2022, **28**, e202103860.
- A. L. Black Ramirez, Z. S. Kean, J. A. Orlicki, M. Champhekar, S. M. Elsakr, W. E. Krause and S. L. Craig, *Nat. Chem.*, 2013, **5**, 757–761.
- H. Zhang, F. Gao, X. Cao, Y. Li, Y. Xu, W. Weng and R. Boulatov, *Angew. Chem., Int. Ed.*, 2016, **55**, 3040–3044.
- H. Traeger, D. J. Kiebala, C. Weder and S. Schrettl, *Macromol. Rapid Commun.*, 2021, **42**, 2000573.
- S. He, M. Stratigaki, S. P. Centeno, A. Dreuw and R. Göstl, *Chem. Eur. J.*, 2021, **27**, 15889–15897.
- J. Zhou, T.-G. Hsu and J. Wang, *Angew. Chem., Int. Ed.*, 2023, **62**, e202300768.
- S. Aydonat, A. H. Hergesell, C. L. Seitzinger, R. Lennarz, G. Chang, C. Sievers, J. Meisner, I. Vollmer and R. Göstl, *Polym. J.*, 2024, **56**, 249–268.
- D. Yildiz, R. Göstl and A. Herrmann, *Chem. Sci.*, 2022, **13**, 13708–13719.
- Z. Shi, Y. Hu and X. Li, *J. Controlled Release*, 2024, **365**, 259–273.
- C. E. Diesendruck, B. D. Steinberg, N. Sugai, M. N. Silberstein, N. R. Sottos, S. R. White, P. V. Braun and J. S. Moore, *J. Am. Chem. Soc.*, 2012, **134**, 12446–12449.
- C. Nagamani, H. Liu and J. S. Moore, *J. Am. Chem. Soc.*, 2016, **138**, 2540–2543.
- Y. Hu, L. Wang, I. Kevlishvili, S. Wang, C.-Y. Chiou, P. Shieh, Y. Lin, H. J. Kulik, J. A. Johnson and S. L. Craig, *J. Am. Chem. Soc.*, 2024, **146**, 10115–10123.
- A. Piermattei, S. Karthikeyan and R. P. Sijbesma, *Nat. Chem.*, 2009, **1**, 133–137.
- P. Michael and W. H. Binder, *Angew. Chem., Int. Ed.*, 2015, **54**, 13918–13922.
- Y. Sha, Y. Zhang, E. Xu, C. Wayne McAlister, T. Zhu, S. L. Craig and C. Tang, *Chem. Sci.*, 2019, **10**, 4959–4965.
- A. Levy, R. Feinstein and C. E. Diesendruck, *J. Am. Chem. Soc.*, 2019, **141**, 7256–7260.
- M. Di Giannantonio, M. A. Ayer, E. Verde-Sesto, M. Lattuada, C. Weder and K. M. Fromm, *Angew. Chem., Int. Ed.*, 2018, **57**, 11445–11450.
- H. Shen, M. B. Larsen, A. G. Roessler, P. M. Zimmerman and A. J. Boydston, *Angew. Chem., Int. Ed.*, 2021, **60**, 13559–13563.



24 K. Imato, A. Irie, T. Kosuge, T. Ohishi, M. Nishihara, A. Takahara and H. Otsuka, *Angew. Chem., Int. Ed.*, 2015, **54**, 6168–6172.

25 T. Yamamoto, A. Takahashi and H. Otsuka, *RSC Mechatnochemistry*, 2024, **1**, 63–68.

26 I. M. Klein, C. C. Husic, D. P. Kovács, N. J. Choquette and M. J. Robb, *J. Am. Chem. Soc.*, 2020, **142**, 16364–16381.

27 R. T. O'Neill and R. Boulatov, *Nat. Rev. Chem.*, 2021, **5**, 148–167.

28 H. Hu, Z. Ma and X. Jia, *Mater. Chem. Front.*, 2020, **4**, 3115–3129.

29 K. L. Berkowski, S. L. Potisek, C. R. Hickenboth and J. S. Moore, *Macromolecules*, 2005, **38**, 8975–8978.

30 T. J. Kucharski, Z. Huang, Q.-Z. Yang, Y. Tian, N. C. Rubin, C. D. Concepcion and R. Boulatov, *Angew. Chem., Int. Ed.*, 2009, **48**, 7040–7043.

31 C. Lupfer, S. Seitel, O. Skarsetz and A. Walther, *Angew. Chem., Int. Ed.*, 2023, **62**, e202309236.

32 Z. J. Wang, J. Jiang, Q. Mu, S. Maeda, T. Nakajima and J. P. Gong, *J. Am. Chem. Soc.*, 2022, **144**, 3154–3161.

33 G. Kim, Q. Wu, J. L. Chu, E. J. Smith, M. L. Oelze, J. S. Moore and K. C. Li, *Proc. Natl. Acad. Sci. U. S. A.*, 2022, **119**, e2109791119.

34 S. Huo, P. Zhao, Z. Shi, M. Zou, X. Yang, E. Warszawik, M. Loznik, R. Göstl and A. Herrmann, *Nat. Chem.*, 2021, **13**, 131–139.

35 Z. Shi, Q. Song, R. Göstl and A. Herrmann, *Chem. Sci.*, 2021, **12**, 1668–1674.

36 Z. Shi, Q. Song, R. Göstl and A. Herrmann, *CCS Chem.*, 2021, **3**, 2333–2344.

37 S. Jung and H. J. Yoon, *Angew. Chem., Int. Ed.*, 2020, **59**, 4883–4887.

38 T. Zeng, L. A. Ordner, P. Liu and M. J. Robb, *J. Am. Chem. Soc.*, 2024, **146**, 95–100.

39 Y. Yao, M. E. McFadden, S. M. Luo, R. W. Barber, E. Kang, A. Bar-Zion, C. A. B. Smith, Z. Jin, M. Legendre, B. Ling, D. Malounda, A. Torres, T. Hamza, C. E. R. Edwards, M. G. Shapiro and M. J. Robb, *Proc. Natl. Acad. Sci. U. S. A.*, 2023, **120**, e2309822120.

40 X. Hu, T. Zeng, C. C. Husic and M. J. Robb, *ACS Cent. Sci.*, 2021, **7**, 1216–1224.

41 T. Zeng, X. Hu and M. J. Robb, *Chem. Commun.*, 2021, **57**, 11173–11176.

42 D. Campagna and R. Göstl, *Angew. Chem., Int. Ed.*, 2022, **61**, e202207557.

43 B. E. F. Ekbrant, A. L. Skov and A. E. Daugaard, *Macromolecules*, 2021, **54**, 4280–4287.

44 M. Muuronen, P. Deglmann and Ž. Tomović, *J. Org. Chem.*, 2019, **84**, 8202–8209.

45 F. I. Altuna, C. E. Hoppe and R. J. J. Williams, *Eur. Polym. J.*, 2019, **113**, 297–304.

46 S. Aydonat, D. Campagna, S. Kumar, S. Storch, T. Neudecker and R. Göstl, *J. Am. Chem. Soc.*, 2024, **146**, 32117–32123.

47 C. Pratley, S. Fenner and J. A. Murphy, *Chem. Rev.*, 2022, **122**, 8181–8260.

48 J. Davies, S. P. Morcillo, J. J. Douglas and D. Leonori, *Chem. Eur. J.*, 2018, **24**, 12154–12163.

49 A. L. J. Beckwith, C. J. Easton and A. K. Serelis, *J. Chem. Soc. Chem. Commun.*, 1980, 482–483.

50 M. Newcomb, T. M. Deeb and D. J. Marquardt, *Tetrahedron*, 1990, **46**, 2317–2328.

51 R. T. McBurney and J. C. Walton, *J. Am. Chem. Soc.*, 2013, **135**, 7349–7354.

52 M. K. Beyer, *J. Chem. Phys.*, 2000, **112**, 7307–7312.

53 P. A. May, N. F. Munaretto, M. B. Hamoy, M. J. Robb and J. S. Moore, *ACS Macro Lett.*, 2016, **5**, 177–180.

54 K. Shimizu, O. Yano, Y. Wada and Y. Kawamura, *Polym. J.*, 1973, **5**, 107–109.

55 B. C. Verma and S. Kumar, *Analyst*, 1974, **99**, 498–502.

